Title: Re-coding of G protein-coupled receptor signaling enables emergent cellular behavior.

Authors: Farhad Dehkhoda[1]†, Mitchell T. Ringuet[2]†, Emily A. Whitfield[3], Keith Mutunduwe[1], Cameron J. Nowell[3], Desye Misganaw[1], Zheng Xu[3], Akhter M. Hossain[4], Linda J. Fothergill[2]‡, Stuart J. McDougall[4], John B. Furness[2,4]*, Sebastian G.B. Furness[1,3]*

Affiliations:

[1]School of Biomedical Sciences, The University of Queensland; Brisbane, Australia.

[2]Department of Anatomy & Physiology, University of Melbourne; Melbourne, Australia.

[3]Monash Institute of Pharmaceutical Sciences; Melbourne, Australia.

[4]Florey Institute of Neuroscience and Mental Health, University of Melbourne, Melbourne, Australia.

†These authors contributed equally to this work

*Corresponding author. Email: j.furness@unimelb.edu.au (J.B.F.); s.furness@uq.edu.au (S.G.B.F)

‡Present address: Walter and Eliza Hall Institute, Melbourne, Australia

Summary:

All cells face the challenge of integrating multiple extracellular signals to produce relevant physiological responses. Different combinations of G protein-coupled receptors, when co-expressed, can lead to distinct cellular outputs, yet the molecular basis for this co-operativity is controversial. One such interaction is the reversal, from inhibition to excitation, at the dopamine D2 receptor in the ghrelin receptor's presence, relevant for defecation control. Here we demonstrate that this reversal of dopamine D2 activity, to excitatory, occurs through a dominant switch in downstream signaling. This dominant switch, mediated by downstream signaling, enables fidelity in cellular responses not possible under alternative models, and provides an explanation for previously unresolved observations. Importantly, the switch in D2 signaling does not require ghrelin receptor agonism, rather its constitutive activity, thus accounting for the importance of central nervous system-ghrelin receptor in the absence of endogenous ligands. This re-coding has important implications for our understanding of how atypical receptor pharmacology can occur as well as how sequential signaling at individual neurons may be encoded to produce new outputs.

Introduction:

How cells interpret the multitude of cues they receive from the extracellular environment to produce the appropriate physiological response is still being elucidated. Much of neuronal signaling requires the coordination of outputs from multiple G protein-coupled receptors (GPCRs) and ion channels. This presents an immediate challenge to neurons because, while the vast majority of GPCRs perform non-overlapping physiological functions, a typical neuron expresses about 80 different GPCRs[1,2], yet these couple to a limited palette of primary transducers[3]. At the molecular level, how the activity of different GPCRs is coded to produce distinct cellular, and thus physiological, outputs is contentious [4,5]. The Rhodopsin-like Class A are the largest GPCR sub-family[6], with the majority binding their ligands in the transmembrane bundle and exhibiting a common activation mechanism[7]. While class A GPCRs do not have an absolute requirement for dimerization for function[8–10], there is a substantial amount of evidence that they can form dimers and higher order oligomers[11]. This has been proposed as a mechanism to explain atypical receptor pharmacology and physiology. Some have cast doubt on this model, highlighting that most studies on GPCR dimerization rely on overexpression with reported heterodimers a possible product of receptor crowding and random collisions[4,5], but there is little data to support alternatives. We[12,13] and others[14], have shown that a subset of neurons that use dopamine as a neuromodulator at the dopamine D2 receptor (DRD2) also express the ghrelin receptor (GHSR), both Rhodopsin-like GPCRs. At these GHSR expressing neurons, dopamine displays an atypical excitatory response[15]. The DRD2 is typically coupled to Gαi/o[16,17] isoforms, and in most neurons DRD2 activation promotes release of Gαi/o associated Gβγ subunits which open G protein-coupled inwardly rectifying potassium (GIRK) channels leading to membrane hyperpolarization and reduced excitability[18]. GHSR, on the other hand, is best characterized as coupling to Gαq/11 isoforms, which, when activated stimulate phospholipase C (PLC) activity[19]. In neurons, the coordinated effect of phosphatidylinositol 4,5-bisphosphate depletion and release of calcium from intracellular stores (via inositol-3-phophate (IP3) leads to M-type potassium channel closure and subsequent membrane depolarization[20]. Thus, in GHSR expressing neurons of the lumbrosacral defecation center, dopamine's excitatory activity at DRD2 is more typical of Gαq/11 coupling, rather than Gαi/o coupling, where Gαi/o coupling is thought to be the predominant signaling pathway from DRD2[17]. We therefore sought to characterize, at the cellular and mechanistic level, how and why DRD2 signaling in the presence of GHSR is re-coded, which is informative of atypical receptor physiology more broadly.

Results:

DRD2 and GHSR are functionally equivalent in the same neurons in the lumbosacral spinal cord

We have previously shown that dopamine and GHSR agonists, acting on spinal defecation centers, are capable of eliciting colorectal contractile activity [12,21,22]. While DRD2 appears to be a physiologically relevant regulator for co-ordination of voluntary defecation in the spinal defecation center [15], GHSR antagonism can block this effect [12,21], which is supported by recent work of Sawamura et. al. [23]. We have also shown that, in spinal defecation center neurons in neonatal rats and adult mice, ~85% respond to dopamine with ~25% exhibiting typical inhibitory responses and ~60% an atypical excitatory response [13]. In defecation center neurons from the same animals ~75% are excited by GHSR activation by capromorelin [13] and the excitatory effect of dopamine is blocked by GHSR antagonism [13]. In defecation center neurons that are excited by dopamine, we can restimulate the same cells with dopamine [13]. When we performed similar experiments with dopamine followed by the GHSR agonist capromorelin, we found that both (Fig 1A-C) neurons from neonatal rat identified by retrograde tracing (Fig 1D & E) and spinal defecation neurons in adult DRD2 reporter mice (Fig 1F) that were excited by dopamine were also excited by GHSR agonism. This indicated that these receptors operate in a functionally similar manner in the same

cells of the spinal defecation center providing support for our previous data on functional interaction between these receptors in spinal defecation neurons [13] and our whole animal data on colonic motility [15].

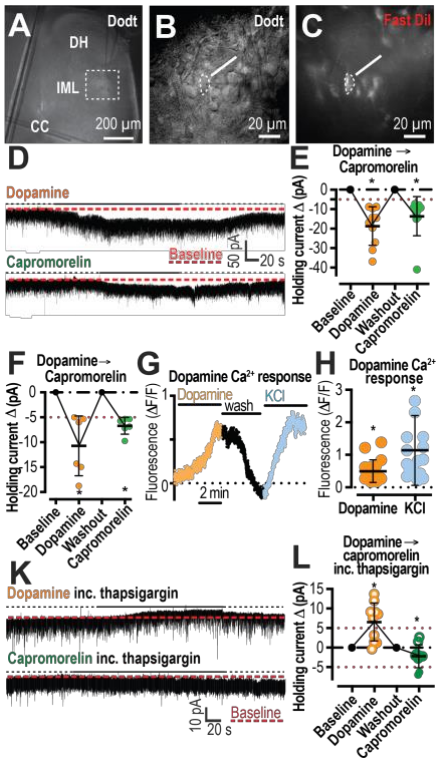

Fig. 1. Activation of either DRD2 or GHSR on spinal defecation center neurons is excitatory but is differentially affected by calcium store depletion. *(**A**) Representative Dodt gradient contrast image of a 300 µm coronal lumbosacral spinal cord slice (rat). Dashed box is recording region r; IML: intermediolateral nucleus; CC: central canal; DH: dorsal horn. (**B, C**) Example of a recorded Fast DiI-retrogradely labeled parasympathetic preganglionic neuron (PPN, dashed line and arrow). (**D**) Inward currents (excitation), in current clamp (all experiments $V_{Holding}$ –60 mV, red-dashed line) in a PPN following 30 µM dopamine and 10 nM capromorelin wash on (solid line: drug exposure period; dashed line: wash on/off). (**E**) Change in inward currents in the same PPNs with successive dopamine (30 µM) and capromorelin (10 nM) applications, n=10 rats, 15 neurons. (**F**) Changes in holding current following dopamine (30 µM) and capromorelin (10 nM) wash on in the same DRD2 neurons from DRD2 reporter mice (n=3 mice, 6 neurons). Mean ± SD, paired student's t-test, *, p<0.05. (**G**) Representative fluorescence trace of DRD2 neuron showing Ca^{2+} responses following dopamine (30 µM; orange) and KCl (75 mM). (**H**) Peak Ca^{2+} fluorescence following dopamine (30 µM) and KCl (75 mM), n = 4 mice, 18 neurons. (**K**) Representative DRD2 neuron generating a typical outward current (inhibition), following 30 µM dopamine in the presence of thapsigargin (1 µM; top). Bottom trace: no change in holding current following 10 nM capromorelin wash on in the presence of 1 µM thapsigargin. (**L**) Dopamine (30 µM; orange) generates outward currents, while capromorelin (10 nM; green) exhibited reduced inward currents in the presence of thapsigargin (1 µM) in the same PPN. Red dashed lines at -5 pA and 5 pA are deemed excitatory and inhibitory thresholds. Closed circles: D2R neuron where inward current >-5 pA; open circle:neuron with no change or an outward current following drug wash on (< -5 pA). All data are mean ± SD, paired student's t-test, peak of drug response delta holding I (pA) /washout, * p<0.05*

Dopamine-induced excitation of DRD2 on mouse lumbosacral spinal cord neurons is reversed with the depletion of intracellular calcium.

Based on previous reports [14,24] and the accepted mechanism of GPCR-dependent neuronal depolarization (e.g. [25]), we hypothesized that intracellular Ca^{2+} mobilization ($_i[Ca^{2+}]$) in *Drd2* neurons in the spinal defecation center was at least in part responsible for the excitation we observed. We identified *Drd2* positive neurons in the spinal defecation center using a drd2-tdTomato reporter mouse and incubated coronal slices in Calbryte 520AM for $_i[Ca^{2+}]$ imaging (Fig. S1). Our results revealed that $_i[Ca^{2+}]$ mobilization occurred in *Drd2* neurons following dopamine (30 μM) and KCl (75 mM) wash on (Fig. 1G, H). $_i[Ca^{2+}]$ store depletion using thapsigargin reversed the excitatory effect of dopamine at DRD2 and reduced capromorelin's excitatory effect (Fig. 1K, L). Thus, DRD2 activation still produced an electrophysiologically measurable, but reversed, output, whereas GHSR effects were largely blocked. These findings indicate that DRD2 and GHSR have different primary coupling; that the subsequent pathway leading to neuronal excitability is only partly shared; and that these receptors can operate independently in these neurons.

GHSR leads to potent re-coding of cellular responses to DRD2 activation in recombinant cell lines

The above observations in native cells indicated that DRD2 activity had been re-coded from an inhibitory to an excitatory output. Our previous data indicate that this re-coding was blocked by GHSR antagonism [13] and required $_i[Ca^{2+}]$ mobilization (Fig. 1L). Previous studies have suggested that re-coding of DRD2 responses result from a dimerization-dependent switch in primary transducer [14], which *is inconsistent with* our above data. We therefore next investigated this in controlled stable cell lines, in which genes for either receptor were present as single copies, resulting in moderate, rather than high receptor expression (Fig. 2A, B, supp Fig. 2J, K). The functional interaction that we observed in spinal neurons was preserved in transfected cells, with atypical DRD2 signaling occurring due to the presence of GHSR (Fig. 2C-D, Supp 2A, L). In the absence of GHSR, dopamine (Fig. 2C, D, G) elicited a mean calcium peak of 3.8% of ionomycin, which increased to a mean of 32% in the presence of GHSR ($logEC_{50}$ -8.3, ~5 nM, Fig. 2D, Supp 2C). The potency of dopamine to elicit a calcium response was very close to that for inhibition of forskolin mediated cAMP (~11nM, Fig. 2J), suggesting a similar ability to engage the transducer(s) responsible for each pathway. A similar effect was obtained with the DRD2-preferring agonist pramipexole (supp Fig 2A, D, E , H , I), and we observed that the presence of either receptor does not alter the cell surface expression of the other (Fig. 2A-B, Supp 2J, K). The magnitudes and kinetic differences of calcium release from DRD2 and GHSR activation were consistent with different pathways to $_i[Ca^{2+}]$ mobilization (Fig. 2C-F). Although $_i[Ca^{2+}]$ downstream of DRD2 was GHSR dependent (Fig. 2C-D), cAMP inhibition was not, shown by the presence of GHSR having no statistically significant or biologically relevant effect on the ability of DRD2 ligands to inhibit the activity of forskolin-stimulated adenylate cyclase (Fig. 2I, J, Supp 2H, I). These results suggest that GHSR provides a dominant second messenger switch for DRD2 in recombinant cell lines (as it does in native cells), consistent with a switch downstream of DRD2's primary transducer.

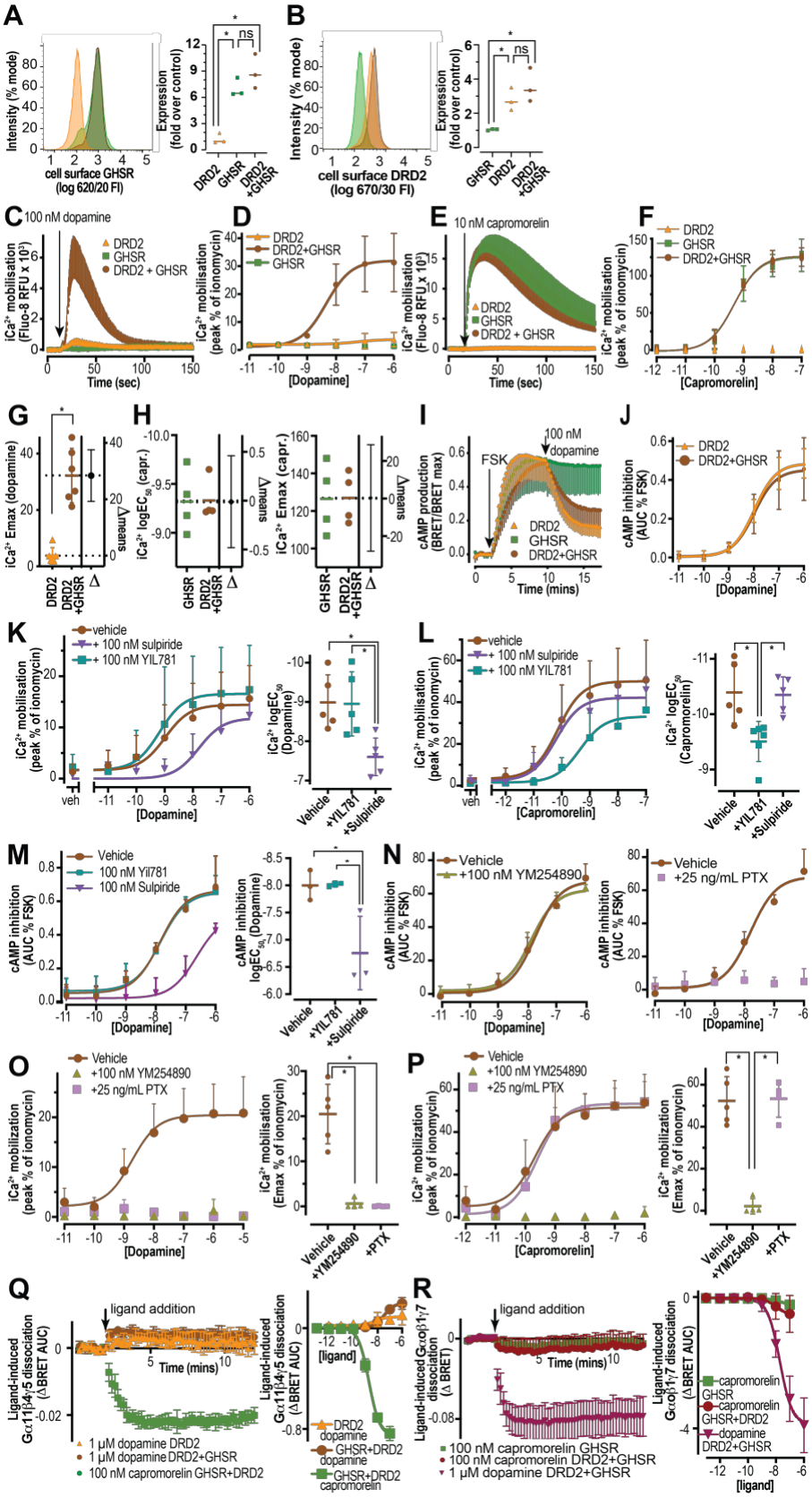

Fig. 2. GHSR provides a pharmacological switch for DRD2 in recombinant cell lines but pathways from GHSR and DRD2 are unique. *(**A,B**) Cell surface expression is not altered by co-expression. Cell surface expression of GHSR (**A**) and DRD2 (**B**) in single copy stably transfected flpIN CHO cell lines using flow cytometry and pooled (fold over control), respectively, in DRD2 (orange, n=3), GHSR (green, n=3) and DRD2+GHSR (brown, n=3). (**C**) GHSR expression is permissive for intracellular* $_i[Ca^{2+}]$ response *of DRD2. Calcium increase (raw RFU) is seen*

*following application of 100 nM dopamine in DRD2+GHSR-transfected cells (brown), but is minimal in DRD2 alone cells (orange) and undetectable in GHSR alone cells (green) alone (n=5). (**D**) $_i[Ca^{2+}]$ quantified as a peak % of ionomycin following dopamine application in DRD2 (orange, n=5), GHSR (green, n=5), and DRD2+GHSR (brown, n=5) transfected cells. (**E**) DRD2 does not change coupling of GHSR to calcium. Ca^{2+} increase following application of 10 nM capromorelin in DRD2+GHSR (brown) and GHSR (green) but is absent in DRD2 (orange) transfected cells (n=5). (**F**) $_i[Ca^{2+}]$ quantified as a peak % of ionomycin following capromorelin application in DRD2 (orange, n=5), GHSR (green, n=5), and DRD2 + GHSR (brown, n=5) transfected cells. (**G,H**) Quantification of EC_{50} and E_{max} of $_i[Ca^{2+}]$ in DRD2 (orange) and DRD2+GHSR (brown) transfected cells following dopamine (**G**) or capromorelin (Capr., **H**) application, based on data in (**D and E**). (**I**) GHSR does not alter DRD2 coupling to cAMP inhibition. Forskolin (FSK; 3 μM) mediated increase of cAMP (BRET/BRET max) which is reduced by dopamine (100 nM) in cells transfected with DRD2+GHSR (brown) or with DRD2 (orange), n=5 but not GHSR alone. (**J**) quantification using area under the curve (AUC) % of FSK as concentration response to dopamine. (**K, L**) The effect of DRD2 preferring antagonist, sulpiride and GHSR antagonist, YIL781 on dopamine (**K**) and capromorelin (**L**) dependent $_i[Ca^{2+}]$, concentration-response curves of peak % ionomycin response with quantified EC_{50} (n=5). (**M**) Reduction with DRD2 preferring antagonist, sulpiride and no effect of GHSR antagonist, YIL781 on dopamine-dependent inhibition of cAMP production, concentration-response curves AUC % inhibition of FSK response with quantified EC_{50} with (n=5). (**N**) The effect of $Ga_{q/11}$ (YM254890, left panel) or $Ga_{i/o}$ (PTX, pertussis toxin) inhibition on dopamine-dependent inhibition of cAMP production, concentration-response curves AUC % inhibition of FSK response (n=3). (**O, P**) The effect of $Ga_{q/11}$ (YM254890) or $Ga_{i/o}$ (PTX) inhibition on dopamine- (**O**) or capromorelin- (**P**) dependent $_i[Ca^{2+}]$, as concentration-response curves peak % of ionomycin response with quantified E_{max} (n=5). (**Q**) The presence of GHSR is not permissive for DRD2 coupling to $Ga_{11}/\beta4\gamma5$ using TRUPATH G protein dissociation assay, left kinetic traces of BRET change in response to saturating ligand and right concentration response curves. (**R**) The presence of DRD2 is not permissive for GHSR coupling to $Ga_o/\beta1\gamma7$ using a TRUPATH G protein dissociation assay, left kinetic traces of BRET change in response to saturating ligand and right concentration response curves. All data are mean ± SD or mean +SD; * $p<0.05$; ns, not significant, one-way ANOVA or unpaired t-test, with estimation plot.*

GHSR and DRD2 have independent signaling pathways in recombinant cell lines.

Because our data on second messenger signaling is consistent with unchanged DRD2 primary transducer coupling in the presence of GHSR, we sought to meticulously characterize this coupling. We began by examining the nature of the re-coding at a receptor-level. In cells containing GHSR and DRD2, antagonism of DRD2 blocks dopamine induced $_i[Ca^{2+}]$ mobilization (Fig. 2K) and reduces cAMP inhibition (Fig. 2M), producing comparable 1.38 and 1.24 log reductions in mean EC_{50}s, but has no effect on GHSR $_i[Ca^{2+}]$ mobilization (capromorelin stimulation, Fig. 2J). Comparable data was seen for pramipexole and ghrelin (Supp Fig. 3A, B, E). Furthermore, GHSR blockade with YIL-781 does not affect DRD2 calcium coupling (Fig. 2K) or cAMP inhibition (Fig. 2M) and produces an expected 0.9 log right-shift in $_i[Ca^{2+}]$ mobilization induced by capromorelin (Fig. 2L), which was comparable for ghrelin (Supp Fig 3C, D). While YIL-781 is reported to be a GHSR inverse agonist, Mende et al. [26] report this to be a weak partial agonist for Gαq/11 in highly coupled systems. Taken together these data are consistent with a dominant second messenger switch of DRD2 provided by GHSR rather than a change in primary transducer via receptor dimerization. Therefore, we sought to understand the involvement of Gαi/o, DRD2's typical coupling partner, and Gαq/11, the typical partner for GHSR, in $_i[Ca^{2+}]$ mobilization. Inhibition of either Gαi/o with pertussis toxin (PTX) or Gαq/11 with YM254890 ablated dopamine (Fig 2O) and pramipexole (Supp Fig 3I, J) dependent $_i[Ca^{2+}]$ mobilization in the GHSR plus DRD2 expressing cell-line, indicating that *both* Gαi/o and Gαq/11 are essential for DRD2-dependent $_i[Ca^{2+}]$

mobilization. By contrast Gαq/11 inhibition with YM254890 had no detectable effect on dopamine (Fig 2N) or pramipexole (Supp Fig 3G) induced inhibition of cAMP production, while, as expected, this cAMP response was completely ablated by PTX (Fig 2N and Supp Fig 3H). Capromorelin (Fig 2P) and ghrelin (Supp Fig 3K, L) dependent $_i[Ca^{2+}]$ mobilization was unaffected by inhibition of Gαi/o with PTX but was undetectable when cells were pre-treated with YM254890. We also used the TRUPATH system [27] to measure whether we could detect a change in preference for coupling to these exogenous G protein sensors. Although DRD2 coupled well to Gαo (Fig 1R, Supp Fig 3O, P) and GHSR to Gα11 (Fig 1Q, Supp Fig 3M, N), our results revealed that the co-expression of both receptors was not permissive for either receptor to couple to its non-preferred partner. Together these data are consistent with there being no change in the primary coupling of either receptor to their preferred Gα partner in the presence of the other receptor and with a co-operative effect of Gαi/o activation (downstream of DRD2) with basal Gαq/11 activity.

No evidence for GHSR and DRD2 direct interaction in recombinant cell lines.

Our interpretation of the reversal of neuronal activity in the presence of GHSR blockade, and the molecular pharmacological analysis, is of a second messenger interaction downstream of DRD2 and GHSR. This dominant switch in second messenger coupling could, nonetheless, be attributed to receptor dimerization. Using directly conjugated antibodies, we performed qualitative deconvolution microscopy to examine the distributions of GHSR and DRD2 (Fig 3A, B, Supp Fig 4 A-C). Although we observed a degree of overlapping signal, for the most part this staining methodology did not support a general co-localization of the two receptors. As an alternative approach, we performed live-cell saturation binding to measure an allosteric effect of one receptor on the other. Both DRD2 and GHSR are essentially transmembrane bundle only receptors, with ligand binding pockets in the transmembrane bundle. A dimerization-dependent switch in DRD2 primary coupling would be expected to involve transmembrane domain allostery with ligand binding co-operativity viewed as the strongest evidence for heterodimers [28]. Based on the structure of DRD2 bound to haloperidol (6LUQ[29]) we reasoned that the haloperidol core could be extended to allow fluorophore conjugation (sulfo-Cy5) to generate a DRD2-preferring fluorescent ligand (shown in Fig 3C, left panel, orange:haloperidol, black:linker, red:sulfo-Cy5, compound name – ZX-1, Supp Fig. 4D). We then used this compound to perform saturation binding on cells expressing DRD2 alone or DRD2 plus GHSR (Fig 3C). No difference in DRD2 affinity for this ligand in the absence or presence of GHSR (Fig 3C, Supp Fig 4E, F) was detected and the binding data reported the same DRD2 receptor number (Fig 3C, Supp Fig 4E, F), independent of GHSR expression, consistent with our flow cytometry results (Fig 2B). Similarly, our published fluorescent GHSR ligand (ghrelin:AF568[30]) could not detect any effect of DRD2 expression on either the affinity of GHSR for this ligand or the number of available GHSRs at the cell surface (Fig 3D, Supp Fig. 4G, H, consistent with Fig 2A). Moreover, saturating concentrations of unlabeled haloperidol had no detectable effect on the binding of ghrelin:AF568 to GHSR (Fig 3E, Sup Fig. 4J) and nor did unlabeled ghrelin affect the binding of ZX-1 to DRD2 (Fig 3F, Supp Fig. 4I), indicating no functionally detectable allosteric interaction between DRD2 and GHSR in these single-gene-copy cells. As these fluorescent ligands provide chemically defined, singly labeled tools where the fluorophore will be very close to the receptor binding pocket when bound, we reasoned that these might be suitable for fine-grained analysis of the distribution of GHSR and DRD2 by super-resolution microscopy. We performed staining and fixation of these cells prior to imaging using STochastic Optical Reconstruction Microscopy (STORM) which were processed, drift-corrected and channel aligned to yield images (vector maps) with effective xy resolutions of 15 nm (Fig 3G). Visual inspection suggested almost none of the localized ZX-1 and ghrelin:AF568 were within the distance range expected for DRD2:GHSR dimerization (Fig 3G). We performed analysis using direct measurement of nearest neighbor distance of ghrelin:AF568 to ZX-1 (3G, bottom panel), where ~ 2% of all measurements were less than our generous cut-off for

dimerization of 25 nm (3x receptor diameter plus allowance for ligand flexibility). This supports the notion that DRD2 and GHSR do not undergo significant heteromerization in these single-copy cells, however at higher receptor densities may place receptors near enough to allow resonance energy transfer using standard fusion protein or antibody methods providing a potential explanation for the discrepancy between our observation and those of others. As a control, Fig 3H shows the localization of ghrelin:AF568 compared to a direct conjugate anti-FLAG:AF647, directed toward the N-terminal tag of the ghrelin receptor. Visual inspection suggested some overlap of signal. Direct nearest neighbor measurements show >30% of all measurements were within 60 nm (1x receptor plus antibody size plus unstructured n-terminus of GHSR plus allowance for ghrelin:AF568 flexibility) for co-binding of ghrelin:AF568 and anti-FLAG:647 to the same receptor. The difference in proximity between fluorescently labelled ligands and a fluorescently labelled ligand and antibody are illustrated in Supp Fig 4K.

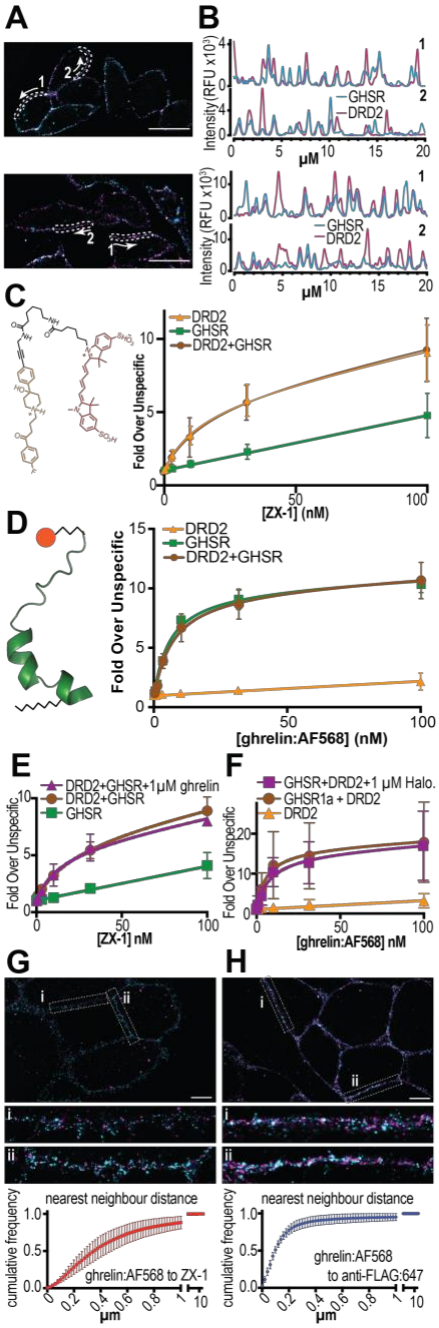

Fig. 3. GHSR and DRD2 appear to be independent at the cell surface in recombinant cell lines. *(A) Representative deconvolution microscopy (n=3) using direct conjugate antibodies directed*

toward n-terminal tags of DRD2 (pseudo-colored in magenta) and GHSR (pseudo-colored in cyan) with effective resolution, xy=160 nm, z=385 nm, scale bars are 20 µM. ***(B)*** *Pixel intensity plots for each channel in the selected membrane segments indicated in* ***(A)****, in the directions of the arrows.* ***(C)*** *Structure of ZX-1, a novel DRD2-preferring fluorescent ligand comprising haloperidol (orange) linked (black) to sulfo-Cy5 (red) and its saturation ligand biding by flow cytometry (no-wash protocol) (n=7).* ***(D)*** *Saturation ligand biding by flow cytometry (no-wash protocol) using ghrelin:AF568, (n=5). Ghrelin:AF568 model at left.* ***(E)*** *Saturation binding by flow cytometry (no-wash protocol) using ZX-1 in the absence and presence of excess (1µM) ghrelin (n=3).* ***(F)*** *Saturation binding by flow cytometry (no-wash protocol) using ghrelin:AF568 in the absence and presence of excess (1µM) haloperidol (n=3).* ***(G, H)*** *Representative super-resolution image using fluorescently labeled DRD2 and GHSR ligand staining* ***(G)*** *and anti-FLAG and GHSR ligand staining* ***(H)*** *of DRD2+GHSR* ***(G)*** *and GHSR* ***(H)*** *cells with an effective resolution xy=15 nm z=42 nm.* ***i*** *and* ***ii*** *show a zoom of areas of the presumptive cell membrane. Bottom shows analysis of pixel-by-pixel minimum distances to nearest neighbor in alternative channel (n=5 independent staining/imaging each with 2-3 images). Scale bar is 5 µM, ghrelin:AF568 is pseudo-colored in cyan, ZX-1 and anti-FLAG:AF647 are pseudo-colored in magenta. All data are mean ± SD.*

DRD2 calcium coupling in neurons in the lumbosacral spinal cord requires PLCβ

A common mechanism whereby GPCRs couple to neuronal depolarization is typified by the ability of Gαq/11 to activate PLCβ which in turn inactivates Kv7 (M-type) potassium channels [25]. Based on the above data, this known mechanism for GPCR-dependent depolarization, and the recent data from the Kostenis' lab [31], demonstrating the requirement for Gαq/11 priming to allow PLCβ to be susceptible to activation by Gαi/o-associated βγ, we propose the model shown in Figure 4A & B. In this model, dopamine causes depolarization due to GHSR-dependent Gαq/11 priming of PLCβ, which enables PLCβ activation by βγ released from DRD2, dominantly inhibiting M-type potassium channels. Contrastingly, in the absence of PLCβ priming and M-channel inhibition, βγ released from DRD2 can dominantly activate GIRK channels, leading to hyperpolarization. Thus, blockade of GHSR and depletion of calcium stores would be expected to lead to DRD2-dependent hyperpolarization (Fig 1 and [13]), the DRD2-dependent increase in iCa^{2+} would be dependent on the presence of GHSR (Fig 2) as well as both Gαi/o and Gαq/11 (Fig 2) but cAMP coupling via Gαi/o would be unaffected by the presence of GHSR (Fig 2) and there would be no requirement for direct receptor:receptor interaction (Fig 3). This model implies that blockade of PLCβ should also lead to DRD2-dependent hyperpolarization and indeed, we observed that in the presence of a PLCβ inhibitor, U73122, dopamine failed to elicit atypical inward excitatory currents, and instead caused typical, outward inhibitory currents (Fig. 4C, D). Consistent with our model, PLCβ inhibition also reduced capromorelin-induced inward, excitatory currents (Fig. 4C, D) an effect that was observed in the same PPN.

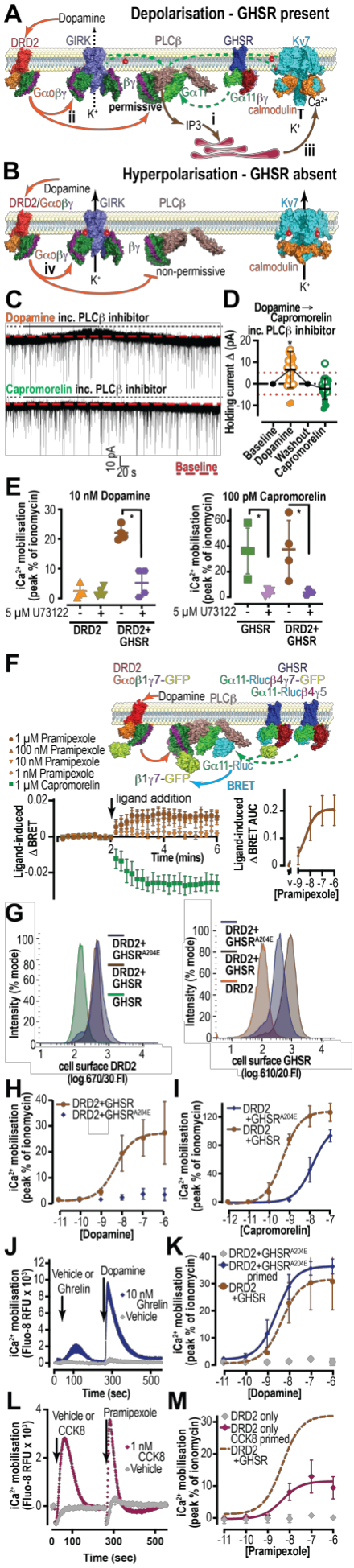
A
Depolarisation - GHSR present
Dopamine
DRD2
GIRK
PLCβ
GHSR
Kv7
Gαoβγ
βγ
Gα11
Gα11βγ
calmodulin
Ca2+
permissive
K+
IP3
i
ii
iii
B
Hyperpolarisation - GHSR absent
DRD2/Gαoβγ
non-permissive
iv
C
Dopamine inc. PLCβ inhibitor
Capromorelin inc. PLCβ inhibitor
10 pA
20 s
Baseline
D
Dopamine → Capromorelin inc. PLCβ inhibitor
Holding current Δ (pA)
Baseline
Dopamine
Washout
Capromorelin
E
10 nM Dopamine
100 pM Capromorelin
iCa2+ mobilisation (peak % of ionomycin)
5 μM U73122
DRD2
DRD2+ GHSR
GHSR
F
DRD2 Gαoβ1γ7-GFP
GHSR Gα11-Rlucβ4γ7-GFP
Gα11-Rlucβ4γ5
Dopamine
PLCβ
Gα11-Rluc
β1γ7-GFP
BRET
1 μM Pramipexole
100 nM Pramipexole
10 nM Pramipexole
1 nM Pramipexole
1 μM Capromorelin
ligand addition
Ligand-induced ΔBRET
Time (mins)
Ligand-induced ΔBRET AUC
[Pramipexole]
G
Intensity (% mode)
DRD2+ GHSRA204E
DRD2+ GHSR
GHSR
DRD2
cell surface DRD2 (log 670/30 FI)
cell surface GHSR (log 610/20 FI)
H
DRD2+GHSR
DRD2+GHSRA204E
[Dopamine]
I
DRD2 +GHSRA204E
DRD2 +GHSR
[Capromorelin]
J
Vehicle or Ghrelin
Dopamine
10 nM Ghrelin
Vehicle
iCa2+ mobilisation (Fluo-8 RFU x 10³)
Time (sec)
K
DRD2+GHSRA204E primed
DRD2 +GHSR
[Dopamine]
L
Vehicle or CCK8
Pramipexole
1 nM CCK8
Vehicle
Time (sec)
M
DRD2 only
DRD2 only CCK8 primed
DRD2 +GHSR
[Pramipexole]

Fig. 4. Model for DRD2 calcium coupling and its testing in neurons in the lumbosacral spinal cord, and the requirement for PLCβ. (A) *Model for the GHSR-dependent switch in DRD2 activity, **(i)** the constitutive activity of GHSR coupled to Gαq/11 primes the system by partly depleting PIP2 from PLCβ, permissive to activation by Gαi/o-associated βγ subunits liberated by DRD2 activation **(ii)** which then fully activates PLCβ, leading to intracellular calcium mobilization and **(iii)** causing a conformational switch in calmodulin at Kv7 (M type) K^+ channels, resulting in channel closure and membrane depolarization. **(B)** In the absence of GHSR-dependent PLCβ priming, DRD2 activation leads to typical Gαi/o associated βγ subunit activation of GIRK channels. **(C)** Representative voltage clamp trace from a PPN generating outward current (inhibition), relative to baseline holding current (red-dashed line, all experiments) following 30 μM dopamine (top) and minimal effect of 10 nM capromorelin (bottom) wash on in the presence of PLCβ inhibitor (10 μM; U73122). Solid line indicates deduced drug effect period. **(D)** Dopamine (30 μM) and capromorelin (10 nM) successive application in the presence of U73122 (10 μM). In most neurons, dopamine caused an outward or no current (open circles). Closed circles indicate neurons where the inward current was >-5 pA. Capromorelin caused no effect or a small outward current in most neurons (open circles) or inward current (closed circles), that was on average smaller than control (Fig 1E) . Red dashed line at -5 pA is deemed the excitatory threshold. Red dashed line at 5 pA is deemed the inhibitory threshold. **(E)** In transfected cells, co-addition of 5μM U73122 (PLCβ inhibitor) largely blocks the ability of dopamine and capromorelin to evoke intracellular Ca^{2+} mobilization, shown as scatter plot of peak calcium (n=5). **(F)** In a TRUPATH assay using $Ga_{11Rluc}/\beta4\gamma5$ in combination with $Ga_o/\beta1\gamma7_{GFP}$, activation of DRD2 with pramipexole results in a BRET increase, while capromorelin stimulation of GHSR causes a decrease (model at top, kinetics at left, concentration-response AUC at right (n=4). **(G)** $GHSR^{A204E}$ (mutant with no constitutive activity) does not alter cell surface expression of DRD2 but is expressed at a lower level compared with wild-type GHSR; cell surface expression of DRD2 and $GHSR^{A204E}$ in single copy stably transfected cell lines using flow cytometry, left expression of DRD2 and right expression of GHSR, in GHSR (green, n=3), GHSR+DRD2 (brown, n=3) and DRD2+ $GHSR^{A204E}$ (purple, n=3) cell lines. **(H)** DRD2 fails to couple to Ca^{2+} in the presence of $GHSR^{A204E}$ following dopamine stimulation **(I)** and capromorelin-induced calcium coupling is right shifted for $GHSR^{A204E}$ compared to conventional GHSR. Mean ± SD. (n=3). **(J)** DRD2 Ca^{2+} coupling is rescued by pre-stimulation of $GHSR^{A204E}$ with low concentration ghrelin. Representative trace showing pre-stimulation with ghrelin (10 nM; blue, n=3) eliciting a small Ca^{2+} response compared to vehicle (gray), followed by dopamine leading to a sharp rise and substantial increase in Ca^{2+} release, compared to vehicle (gray). **(K)** Dose-response relationship of Ca^{2+} increase from dopamine following pre-stimulation with ghrelin (10nM; blue, n=3). **(L)** DRD2 Ca^{2+} coupling in DRD2 only cells is rescued by pre-stimulation of endogenous CCK1-R with low concentration CCK-8. Representative trace showing pre-stimulation with CCK-8 (1 nM; magenta, n=3) eliciting a Ca^{2+} response compared to vehicle (gray), followed by pramipexole leading to a sharp rise and substantial increase in Ca^{2+} release, compared to vehicle (gray). **(M)** Dose-response relationship of Ca^{2+} increase from pramipexole following pre-stimulation with CCK-8 (1 nM; magenta, n=3). Mean ± SD, paired student's t-test **(D)**, one way ANOVA **(E)** * $p<0.05$*

GHSR-dependent coupling of DRD2 to calcium requires GHSR constitutive activity

We sought to confirm integration of DRD2 and GHSR signaling at PLCβ. Consistent with neuronal activity, the PLCβ inhibitor, U73122, blocked both DRD2- and GHSR-dependent Ca^{2+} mobilization in transfected cells (Fig 4G and Supp Fig 5A). Furthermore, when we combined TRUPATH sensors for both Gαo and Gα11, but with the donor Rluc8 only on Gα11 and the acceptor GFP on the Gαo preferred Gγ7, stimulation of DRD2 in cells co-expressing GHSR caused an increase in BRET signal, consistent with an increase in proximity of $G\alpha11_{Rluc8}$ and $G\gamma7_{GFP}$, (Fig 4H). This is consistent with our model where Gα11 and βγ subunits liberated from Gαo converge on PLCβ (Fig

4A and H). Because this integration of signaling and our model requires GHSR constitutive activity, we developed single-gene copy cell lines that co-express DRD2 and the naturally occurring $GHSR^{A204E}$ mutant, which is reported to lack constitutive activity, but is still responsive to ghrelin [32]. This mutant did not alter cell surface expression of DRD2 (Fig 4H, left panel, quantitated Supp 5B) but exhibited 2-fold lower expression compared with the wild-type receptor (Fig 4H, quantitated supp 5B). Co-expression of $GHSR^{A204E}$ with DRD was completely non-permissive for DRD2-dependent calcium mobilization (Fig 4I and Supp Fig 5C), and also displayed reduced responsiveness to capromorelin (Fig 4J) and ghrelin (Supp Fig 5D). Conversely, system priming with an approximate EC_{10} concentration of ghrelin allowed dopamine (Fig 4K, L) and pramipexole (Supp Fig 5E, F) to couple to intracellular calcium mobilization to the same extent as in cells co-expressing wild-type GHSR, supporting the notion that the low-level tonic activation of Gαq/11, downstream of GHSR, is necessary and sufficient for a pharmacological switch in DRD2 behavior. This suggested to us that system priming via another Gαq/11 coupled GPCR may be permissive for DRD2-dependent Ca^{2+} mobilization. These cells express low, but pharmacologically detectable levels of the cholecyctokinin 1 receptor (CCK1R), a typically Gαq/11 coupled GPCR. Priming of DRD2-only expressing cells with a low (1 nM, ~EC_{30}) concentration of CCK-8 led to a recovery in the ability of dopamine to elicit a Ca^{2+} response, with an EC_{50} similar to that seen in cells co-expressing DRD2 with GHSR. This suggests a generalizable effect of Gαq/11 priming on the ability of DRD2 to couple to calcium via Gαi/o.

Discussion

DRD2s are expressed in a subset of neurons throughout the central nervous system, where they participate in a range of different physiologies including motor control, reward (including feeding reward), cognition and, as we and others have recently shown, voluntary defecation [15,23]. These receptors typically act by inhibiting neuronal excitation through coupling to Gαi/o and downstream βγ dependent opening of GIRK channels [18,33]. It has been reported that when DRD2 is associated with the ghrelin receptor, activation of DRD2 causes atypical excitation [14,15,24]. We investigated the molecular mechanism through which this reversal of effect at DRD2 occurs in both transfected cells and native autonomic neurons. Our data supports a model in which the GHSR-dependent switch of DRD2's action from inhibition to excitation depends on the ability of GHSR to tonically activate Gαq/11, such that Gαq/11-activated PLCβ is permissive for DRD2-dependent Gαi/o associated βγ activation. In contrast to previous reports [14,24], we found no evidence for dimerization being associated with the GHSR-dependent switch in DRD2's action. Our results also demonstrate that the re-coding of DRD2 can occur through pre-stimulation of the naturally occurring $GHSR^{A204E}$ mutant that lacks constitutive activity, but is still agonist responsive, with a very low concentration of ghrelin. This enables potent and efficacious coupling of DRD2 to an atypical calcium response. This ability of pre-stimulation of a Gαq/11 coupled receptor to re-code DRD2 response is also true for CCK1R.

These two re-coding effects have broad implications for GPCR biology. Firstly, in the case of GHSR recoding, a variety of observations regarding the ability of GHSR inverse agonists to alter dopaminergic and opioid signaling may be due to the physiological function of GHSR which allows these Gαi/o coupled receptors to have a neuro-excitatory effect. This has important implications for the choice of centrally penetrant GHSR antagonist for treating addiction disorders [34]. Our model also accounts for the previous observation of synergistic effects of DRD2 and GHSR agonists in treating constipation in a preclinical model of Parkinson's Disease[35]. We would propose that Parkinson's Disease-associated chronic-constipation (present in 70-80% of patients[36]) may respond to subtherapeutic doses of capromorelin, which would act to potentiate the normal dopamine-mediated voluntary-defecation response. Another implication of GHSR dependent recoding of DRD2 activity with no change in primary transducer, is that it provides a mechanism for neuronal response fidelity, distinguishing an excitatory input from a Gαi/o coupled receptor (e.g. DRD2 in a

GHSR expressing neuron) from a Gαq/11 coupled receptor (e.g. a muscarinic M1, 3 or 5 input). This mechanism for a fidelity in cellular response, may not be possible under a dimerization model. In this example, both inputs may be expected to cause transient depolarization but because DRD2 activation will also cause a decrease in cellular cAMP, its activation might be expected to reduce after-depolarization events and produce different medium-term changes in gene expression. Secondly, the fact that very low-level pre-stimulation of Gαq/11, through both $GHSR^{A204E}$ and CCK1R, leads to temporary re-coding of the DRD2 response implies a mechanism by which the order of signals arriving at a neuron could be coded to provide a physiologically plastic conditional response. The ability of GHSR to interact with other GPCRs could have implications in their physiological activity with important consequences for learning and memory, metabolic disorders and issues relating to colonic motility. This type of second-messenger convergence provides a model to understand observations such as the melanocortin-4 receptor-dependent reversal of valence that is mediated via the dopaminergic reward pathway [37]. Thus, the ability to re-code GPCR output provides a mechanism by which emergent behavior can arise from a limited palette of transducers.

References and Notes:

1. Hawrylycz, M. J. *et al.* An anatomically comprehensive atlas of the adult human brain transcriptome. *Nature* **489**, 391–399 (2012).

2. Lein, E. S. *et al.* Genome-wide atlas of gene expression in the adult mouse brain. *Nature* **445**, 168–176 (2007).

3. Downes, G. B. & Gautam, N. The G Protein Subunit Gene Families. *Genomics* **62**, 544–552 (1999).

4. Sleno, R. & Hébert, T. E. Shaky ground - The nature of metastable GPCR signalling complexes. *Neuropharmacology* **152**, 4–14 (2019).

5. Lambert, N. A. & Javitch, J. A. CrossTalk opposing view: Weighing the evidence for class A GPCR dimers, the jury is still out. *J Physiology* **592**, 2443–2445 (2014).

6. Fredriksson, R., Lagerström, M. C., Lundin, L.-G. & Schiöth, H. B. The G-protein-coupled receptors in the human genome form five main families. Phylogenetic analysis, paralogon groups, and fingerprints. *Mol Pharmacol* **63**, 1256–1272 (2003).

7. Zhou, Q. *et al.* Common activation mechanism of class A GPCRs. *eLife* **8**, e50279 (2019).

8. Whorton, M. R. *et al.* A monomeric G protein-coupled receptor isolated in a high-density lipoprotein particle efficiently activates its G protein. *Proceedings of the National Academy of Sciences of the United States of America* **104**, 7682–7687 (2007).

9. Ernst, O. P., Gramse, V., Kolbe, M., Hofmann, K. P. & Heck, M. Monomeric G protein-coupled receptor rhodopsin in solution activates its G protein transducin at the diffusion limit. *Proc. Natl. Acad. Sci.* **104**, 10859–10864 (2007).

10. Bayburt, T. H., Leitz, A. J., Xie, G., Oprian, D. D. & Sligar, S. G. Transducin activation by nanoscale lipid bilayers containing one and two rhodopsins. *The Journal of biological chemistry* **282**, 14875–14881 (2007).

11. Gomes, I. *et al.* G Protein-Coupled Receptor Heteromers. *Annual review of pharmacology and toxicology* **56**, 403–425 (2016).

12. Furness, J. B. *et al.* Dopamine and ghrelin receptor co-expression and interaction in the spinal defecation centers. *Neurogastroenterology and motility : the official journal of the European Gastrointestinal Motility Society* e14051 (2020) doi:10.1111/nmo.14051.

13. Ringuet, M. T., Koo, A., Furness, S. G. B., Furness, S. M. J. & Furness, J. B. Sites and mechanisms of action of colokinetics in the lumbosacral defecation centre. *The Journal of Physiology* (2023) doi:10.1113/jp285217.

14. Kern, A., Albarran-Zeckler, R., Walsh, H. E. & Smith, R. G. Apo-ghrelin receptor forms heteromers with DRD2 in hypothalamic neurons and is essential for anorexigenic effects of DRD2 agonism. *Neuron* **73**, 317–332 (2012).

15. Furness, J. B. *et al.* Dopamine and ghrelin receptor co-expression and interaction in the spinal defecation centers. *Neurogastroenterology and motility : the official journal of the European Gastrointestinal Motility Society* e14051 (2020) doi:10.1111/nmo.14051.

16. Montmayeur, J. P. & Borrelli, E. Transcription mediated by a cAMP-responsive promoter element is reduced upon activation of dopamine D2 receptors. *Proc. Natl. Acad. Sci.* **88**, 3135–3139 (1991).

17. Masuho, I. *et al.* Rules and mechanisms governing G protein coupling selectivity of GPCRs. *Cell Rep.* **42**, 113173 (2023).

18. Neve, K. A., Seamans, J. K. & Trantham-Davidson, H. Dopamine Receptor Signaling. *J Recept Sig Transd* **24**, 165–205 (2004).

19. Holst, B., Brandt, E., Bach, A., Heding, A. & Schwartz, T. W. Nonpeptide and peptide growth hormone secretagogues act both as ghrelin receptor agonist and as positive or negative allosteric modulators of ghrelin signaling. *Molecular Endocrinology* **19**, 2400–2411 (2005).

20. Robbins, J., Marsh, S. J. & Brown, D. A. Probing the regulation of M (Kv7) potassium channels in intact neurons with membrane-targeted peptides. *J. Neurosci. : Off. J. Soc. Neurosci.* **26**, 7950–61 (2006).

21. Pustovit, R. V. *et al.* Evidence that central pathways that mediate defecation utilize ghrelin receptors but do not require endogenous ghrelin. *Physiological Reports* **5**, e13385 (2017).

22. Pustovit, R. V., Furness, J. B. & Rivera, L. R. A ghrelin receptor agonist is an effective colokinetic in rats with diet-induced constipation. *Neurogastroenterology and motility : the official journal of the European Gastrointestinal Motility Society* **27**, 610–617 (2015).

23. Sawamura, T. *et al.* Essential roles of the hypothalamic A11 region and the medullary raphe nuclei in regulation of colorectal motility in rats. *Am. J. Physiol.-Gastrointest. Liver Physiol.* **324**, G466–G475 (2023).

24. Kern, A., Grande, C. & Smith, R. G. Apo-Ghrelin Receptor (apo-GHSR1a) Regulates Dopamine Signaling in the Brain. *Frontiers in endocrinology* **5**, 129 (2014).

25. Kosenko, A. *et al.* Coordinated signal integration at the M-type potassium channel upon muscarinic stimulation. *Embo J* **31**, 3147–3156 (2012).

26. Mende, F. *et al.* Translating biased signaling in the ghrelin receptor system into differential in vivo functions. *Proceedings of the National Academy of Sciences* **10**, 201804003 (2018).

27. Olsen, R. H. J. *et al.* TRUPATH, an open-source biosensor platform for interrogating the GPCR transducerome. *Nature chemical biology* **22**, 362 (2020).

28. Birdsall, N. J. M. Class A GPCR heterodimers: evidence from binding studies. *Trends Pharmacol. Sci.* **31**, 499–508 (2010).

29. Fan, L. *et al.* Haloperidol bound D2 dopamine receptor structure inspired the discovery of subtype selective ligands. *Nat Commun* **11**, 1074 (2020).

30. Liu, M. *et al.* Design, synthesis and characterization of a fluorescently labeled functional analog of full-length human ghrelin. *Biochemical and biophysical research communications* **533**, 559–564 (2020).

31. Pfeil, E. M. *et al.* Heterotrimeric G Protein Subunit Gαq Is a Master Switch for Gβγ-Mediated Calcium Mobilization by Gi-Coupled GPCRs. *Molecular Cell* (2020) doi:10.1016/j.molcel.2020.10.027.

32. Pantel, J. *et al.* Loss of constitutive activity of the growth hormone secretagogue receptor in familial short stature. *The Journal of clinical investigation* **116**, 760–768 (2006).

33. Martel, J. C. & McArthur, S. G. Dopamine Receptor Subtypes, Physiology and Pharmacology: New Ligands and Concepts in Schizophrenia. *Front Pharmacol* **11**, 1003 (2020).

34. Gomez, J. L. & Ryabinin, A. E. The Effects of Ghrelin Antagonists [D-Lys3]-GHRP-6 or JMV2959 on Ethanol, Water, and Food Intake in C57BL/6J Mice. *Alcohol.: Clin. Exp. Res.* **38**, 2436–2444 (2014).

35. Chai, X. *et al.* Investigation of nerve pathways mediating colorectal dysfunction in Parkinson's disease model produced by lesion of nigrostriatal dopaminergic neurons. *Neurogastroenterol. Motil.* **32**, e13893 (2020).

36. Fasano, A., Visanji, N. P., Liu, L. W. C., Lang, A. E. & Pfeiffer, R. F. Gastrointestinal dysfunction in Parkinson's disease. *The Lancet. Neurology* **14**, 625–639 (2015).

37. Klawonn, A. M. *et al.* Motivational valence is determined by striatal melanocortin 4 receptors. *J. Clin. Investig.* **128**, 3160–3170 (2018).

38. Anderson, C. R. & Edwards, S. L. Intraperitoneal injections of fluorogold reliably labels all sympathetic preganglionic neurons in the rat. *J. Neurosci. Methods* **53**, 137–141 (1994).

39. Khan, Z. U., Mrzljak, L., Gutierrez, A., Calle, A. de la & Goldman-Rakic, P. S. Prominence of the dopamine D2 short isoform in dopaminergic pathways. *Proc. Natl. Acad. Sci.* **95**, 7731–7736 (1998).

40. Maso, E. D. *et al.* Characterization of signalling and regulation of common calcitonin receptor splice variants and polymorphisms. *Biochemical Pharmacology* **148**, 111–129 (2018).

41. Fyfe, T. J. *et al.* A Thieno[2,3-d]pyrimidine Scaffold Is a Novel Negative Allosteric Modulator of the Dopamine D2 Receptor. *J Med Chem* **62**, 174–206 (2019).

42. Furness, S. G. B. *et al.* Ligand-Dependent Modulation of G Protein Conformation Alters Drug Efficacy. *Cell* **167**, 739-749.e11 (2016).

Acknowledgments:

The authors thank Ben Capuano, Peter Scammells and Rob Lane for their supervision of ZX and Ben Capuano for assistance with preparing methods relating to the compound ZX-1. The authors would like to acknowledge that the present work was conducted on the traditional lands of the Turrbal and Wurundjeri peoples. We would like to thank Dominic Ng, Sean Millard, Wally Thomas, Scott Prosser and Rowan Tweedale for constructive critique of the manuscript. STORM data acquisition was performed at the Queensland Brain Institute's Advanced Microscopy Facility using the SAFe 360; Abbelight, France.

Funding

2021 NHMRC Ideas Grant; 2021/GNT2012657 (SGBF, LJF, JBF)

SGBF is an ARC Future Fellow (FT180100543)

Author contributions

Conceptualization: SGBF, JBF

Methodology: FD, MTR, EAW, CJN, ZX, AMH, SGBF

Investigation: FD, MTR, EAW, KM, DM, JBF, SGBF

Visualization: MTR, FD, CJN, JBF, SGBF

Funding acquisition: SGBF, LJF, JBF

Project administration: SGBF, JBF

Supervision: SGBF, JBF, SJM

Writing – original draft: SGBF, JBF, FD, MTY

Writing – review & editing: FD, MTR, SGBF, JBF

Competing interests None

Data and materials availability All data are available in the main text or the supplementary materials.